Campos Frances, M.; San Millan, A.; Sempere Luna, JM.; Lanza, VF.; Coque, TM.; Llorens, C.; Baquero, F. (2020). Simulating the Influence of Conjugative-Plasmid Kinetic Values on the Multilevel Dynamics of Antimicrobial Resistance in a Membrane Computing Model. Antimicrobial Agents and Chemotherapy. 64(8):1-19. https://doi.org/10.1128/AAC.00593-20

Simulating the Influence of Conjugative Plasmids Kinetic Values on the Multilevel Dynamics of Antimicrobial Resistance in a Membrane Computing Model

Marcelino Campos,[a,c] **Álvaro San Millán,**[a,d,e] **José M. Sempere,**[c] **Val F. Lanza,**[a,f,e] **Teresa M. Coque,**[a,e] **Carlos Llorens,**[b] **Fernando Baquero** [a,e] #

[a]Department of Microbiology, Ramón y Cajal University Hospital, IRYCIS, Madrid, Spain.

[b]Biotechvana, Valencia, CEEI Building, Valencia Technological Park, Paterna, Spain.

[c]Valencian Research Institute for Artificial Intelligence (VRAIN), Universitat Politècnica de València, Spain.

[d]National Center for Biotechnology, (CNB-CSIC), Madrid, Spain.

[e]Network Research Center for Epidemiology and Public Health (CIBERESP), Madrid, Spain.

[f]Bioinformatics Support Unit, IRYCIS, Madrid, Spain.

Running title: Plasmid kinetics in a membrane computing model

#**Address correspondence** to Fernando Baquero, baquero@bitmailer.net

Abstract

Plasmids harboring antibiotic resistance genes differ in their kinetic values as plasmid conjugation rate, segregation rate by incompatibility with related plasmids, rate of stochastic loss during replication, cost reducing the host-cell fitness, and frequency of compensatory mutations to reduce plasmid cost, depending on the cell mutation frequency. How variation in these values influence the success of a plasmid and their resistance genes in complex ecosystems, as the microbiota? Genes are located in plasmids, plasmids in cells, cells in populations. These populations are embedded in ensembles of species in different human hosts, are able to exchange between them bacterial ensembles during cross-infection and are located in the hospital or the community setting, under various levels of antibiotic exposure. Simulations using new membrane computing methods help predict the influence of plasmid kinetic values on such multilevel complex system. In our simulation, conjugation frequency needed to be at least 10^{-3} to clearly influence the dominance of a strain with a resistant plasmid. Host strains able to stably maintain two copies of similar plasmids harboring different resistances, coexistence of these resistances can occur in the population. Plasmid loss rates of 10^{-4} or 10^{-5} or plasmid fitness costs ≥ 0.06 favor the plasmids located in the most abundant species. The beneficial effect of compensatory mutations for plasmid fitness cost is proportional to this cost, only at high mutation frequencies (10^{-3}-10^{-5}). Membrane computing helps set a multilevel landscape to study the effect of changes in plasmid kinetic values on the success of resistant organisms in complex ecosystems.

Introduction

Plasmid kinetics are widely assumed to necessarily influence the spread of antibiotic resistance genes in bacterial populations and ecosystems (1-10). The main parameters that affect plasmid kinetics are: a) the rate of plasmid conjugation/transfer (the rate at which a bacterial cell harboring a conjugative plasmid [donor] transfers this plasmid to a recipient cell; b) the segregation rate due to plasmid incompatibility (considering the number of plasmid genome copies that are stably maintained in a bacterial cell); c) the rate of plasmid cost (the reduction imposed by the presence [and transfer] of a plasmid in the growth rate of the host bacterial cell); d) the rate of plasmid cost compensation (measuring the effect of mutations reducing plasmid cost); e) the frequency of mutational events in the plasmid or bacterial genome; and f) the rate of plasmid loss (the rate at which plasmids are lost during the bacterial replication process).

However, the effects of these changes on the kinetics of plasmid resistance genes among bacterial populations are necessarily influenced by numerous other factors acting in actual biological ecosystems, such as the intestinal microbiota. Of these factors, our previously published studies on modeling by membrane computing (11-13) considered the following: the ecosystem's bacterial composition, the density and replication rate of cells in each species, their mutation frequencies, the content in chromosomal resistance genes, the selection intensity of resistant organisms due to differing antibiotic exposures, the elimination of susceptible bacterial populations by antibiotic treatment, the transmission of resistant bacteria among human hosts in hospital settings under differing admission-discharge rates, cross-colonization, and exposure to various antibiotics, as well as the influence of antibiotic resistance in non-hospitalized individuals who eventually pass through the hospital environment.

Experimentally investigating the influence of changes in plasmid kinetic parameters is extremely difficult and perhaps impossible, under real-world conditions. The research involves a complex, multilevel, multiparametric, and interactive landscape, involving genes, cells, populations, communities, hosts, and factors that influence transmission and selection. However, this problem can be approached using novel computational models integrating within-host and between-host modeling (14,15). Multilevel membrane computing models can provide an ecosystem-like framework composed of discrete independent but interactive units mimicking biological ones in a multi-hierarchical landscape of nested entities (e.g., genes inside plasmids, plasmids inside bacteria, bacteria inside microbiota, microbiota inside hosts, hosts inside the hospital, and interacting with the community) (12).

Membrane computing is conceptually based on complex biological systems, which are characterized by structured nested biological entities than can be conceptualized as separated by "membranes" (16,17). Each genes, plasmids, cells, species, populations, hosts, and compartments where the host is located (such as the community or hospital) is surrounded by "computational membranes" forming a multilevel nested structure, that can be studied by devices such as membrane systems or P systems (12, 13). The P system applied in this study mimics the complex biological landscapes in the computer world. In our model, each of the nested "membrane-surrounded entities" can independently replicate, propagate, become extinct, transfer into other membranes, exchange informative material according to flexible rules, mutate, and be selected by external agents (13). This computational model helps simulate the combined effect of changes in the various parameters, influencing the spread of antibiotic resistance plasmids. This study explores how changes in these parameters influence the spread of antibiotic resistance genes located in plasmids, in bacterial populations, and in microbial

communities composed of different bacterial species, and which are the consequences of this spread. We also explore how these changes and their effects determine the frequency of various clones or species that harbor plasmids with antibiotic resistance genes. A simplified representation of the elements introduced in the membrane computing system is presented in Figure S1 (Supplemental Material).

In summary, we present a number of case studies analyzing the influence of changing plasmid kinetic values on complex hierarchical dynamics of antibiotic resistance in a simulated hospital setting. Most of the computing experiments referred to in this study mimics an evolution of 4.5 years (40,000 1-hour steps). To our knowledge, this is the first study that has addressed the effect of plasmid kinetic parameters in on the structure of multilevel biological systems.

Results

The details and acronyms employed in the model are provided in Materials and Methods. However, to facilitate the understanding of the Results section, Table 1 is presented below.

Table 1

Acronym	Definition	Notes
AbA	Antibiotic A	As aminopenicillins
AbC	Antibiotic C	As 3rd-generation cephalosporins
AbF	Antibiotic F	As fluoroquinolones
AbAR	Plasmid-mediated resistance to AbA	As TEM-1
AbCR	Plasmid-mediated resistance to AbC	As ESBLs
AbFR	Chromosomal fluoroquinolone mutation	As *gyrA* mutation
AbA*R	Chromosomal gene resistance to AbA in *K. pneumoniae*	As SHV-1
PL1	Plasmid 1, originally in an *E. coli* population, with AbAR	Incompatible with PL3
PL3	Plasmid 3, originally in *K. pneumoniae*, AbCR and AbAR	Incompatible with PL1
Ec0	*E. coli* without plasmids, fully susceptible	
EcA	*E. coli* with PL1 AbAR	
EcC	*E. coli* with PL3 AbCR-AbAR	
EcF	*E. coli* with chromosomal AbFR	
EcAC	*E. coli* with PL1 and PL3 AbAR-AbCR	
EcAF	*E. coli* with PL1 AbAR and chromosomal AbFR	
EcCF	*E. coli* with PL3 AbCR-AbAR and chromosomal AbFR	
EcACF	E. coli with PL1 AbAR, PL3 AbCR-AbCR, and AbFR	

118

119 **Influence of plasmid conjugation rates**

120 How to estimate plasmid transfer rates is not a trivial question (18). In this simulation,
121 conjugation rates are expressed as the proportion of donor-recipient contacts that result
122 in a random and reciprocal cell-to-cell *E. coli-K. pneumoniae* plasmid transfer in a
123 given period. For instance, 10^{-6} per hour, indicates that 1 in 100,000 contacts or 1
124 million donor-recipient contacts resulted in random and reciprocal cell-to-cell *E. coli-K.*
125 *pneumoniae* plasmid transfers per hour. Conjugation rates widely differ in different
126 plasmid-host combinations (19-22) and also is heavily influenced by the abundance and
127 well-mixing of interacting bacterial populations (23). Our model included 3 conjugation
128 rates (10^{-3}, 10^{-6}, and 10^{-9}) applicable to plasmids PL1 and PL3, harbored by either *E.*
129 *coli* or *K. pneumoniae*. The rate of spontaneous plasmid loss (segregation) was 10^{-5}, and
130 the mutation frequency for plasmid cost compensatory mutations was 10^{-5} (mutants
131 reduced to one half the cost of harboring plasmids). Other default values are as
132 described in the Materials and Methods section. The results for the various *E. coli*
133 phenotypes emerging from the plasmid transfer and mutational resistance to
134 fluoroquinolones are presented in Figure 1. At first sight, a dramatic effect on the *E. coli*
135 population structure is only observed at high plasmid transfer rates (10^{-3}) (Fig. 1a, 1b).
136 A first selective burst of AbAR (red line) is followed by the AbAR-AbFR phenotype
137 (brown) (due to the mutational evolution to fluoroquinolone resistance of AbAR cells)
138 and by the acquisition of PL1 (AbAR) by the AbFR cells. The acquisition of PL3 from
139 *K. pneumoniae* occurs almost simultaneously (now, AbA*R-AbCR, light blue) and then
140 from AbFR *E. coli* (now, AbAR-AbCR-AbA*R, AbFR, dark blue). Subsequently, the
141 predominant populations are AbFR *E. coli* harboring PL3 (AbCR-AbA*R, AbFR)
142 (green).

143 *K. pneumoniae* is critical at the start of the process by providing the plasmid PL3
144 (AbCR-AbA*R) to *E. coli*; however, most plasmid transfers occur among the *E. coli*
145 bacteria, thereby acquiring most of the antibiotic resistance benefits (Fig. 1c). With
146 medium to low transfer rates, *E. coli* populations appear to remain stable and do not
147 spread significantly in the human host population (lower boxes in Fig. 1a, 1c).
148 Interestingly, a logarithmic representation (Fig. 1b) reveals remarkable differences at
149 the 10^{-6} and 10^{-9} transfer rates in regard to the population structure. At both 10^{-6} and 10^{-9}
150 transfer rates, there is a steady preservation of the fully susceptible *E. coli* population
151 (pink), AbFR *E. coli* (violet) and containing PL1(AbAR) (red), and populations
152 harboring PL1 (AbAR-AbFR) (brown). At the 10^{-6} transfer rate, however, a small part
153 of the *E. coli* population acquires the PL3 plasmid from *K. pneumoniae* (and later from
154 *E. coli*/PL3), giving rise to a constant increase in the phenotypes AbCR-AbA*R (green),
155 AbCR-AbA*R-AbFR (olive green), and AbAR-AbCR-AbA*R, AbFR (dark blue).

156 Even at the 10^{-9} transfer rate, a few *E. coli* capture the PL3 plasmid but are unable to
157 spread AbCR efficiently in the *E. coli* population. The long-term maintenance of *K.*
158 *pneumoniae* with PL3 (olive green) is only assured at low transfer rates (10^{-6}, 10^{-9}),
159 impairing the dominance of resistant *E. coli* populations (Fig. 1d), given that, at high
160 transfer rates, the *E. coli* invade the *K. pneumoniae* cells with plasmid PL1, which
161 might lose their resident PL3 plasmids due to incompatibility.

162

163

164

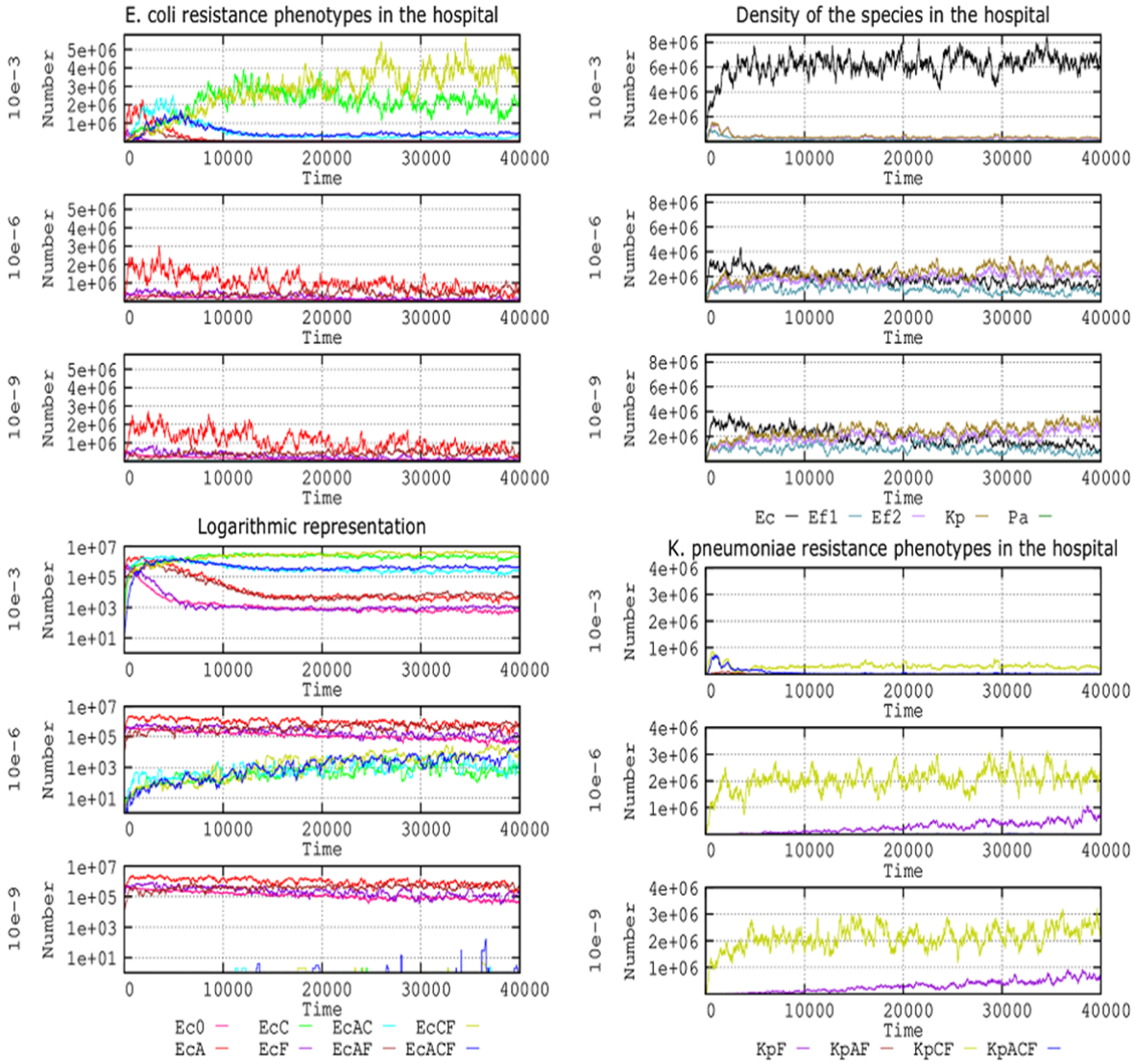

Figure 1: Influence of plasmid conjugation frequency (10^{-3}, 10^{-6}, 10^{-9}) on the evolution of E. coli resistance phenotypes in the hospital. *Upper left: Ec0, susceptible, no resistance plasmids (pink line), EcA, PL1-AbAR (red); EcC, PL3-AbAR-AbCR (light fluorescent green), EcF, AbFR (violet), EcAC, PL1-AbAR plus PL3-AbAR-AbCR, (light blue), EcAF, PL1-AbAR plus AbFR (brown), EcCF, PL3, AbAR-AbCR plus AbFR (olive green), EcACF, PL1-AbAR plus PL3-AbAR-AbCR plus AbFR (dark blue). Lower left: a logarithmic representation of the same resistance phenotypes. Upper right: density of the species E. coli (black line), K. pneumoniae (olive green), ampicillin-R E. faecium (violet), and ampicillin-S E. faecium (blue-green). Lower*

174 *right: detail of the evolution of K. pneumoniae (olive green) and E. faecium. Numbers in*
175 *ordinates are expressed in hecto-cells (one unit=100 cells in the microbiota)*

176

177 **Influence of plasmid incompatibility**

178 Our model included the term "plasmid incompatibility" to explore the segregation of
179 replicons sharing similar partitioning (par) loci, thus leading to mutual interference (24).
180 We examined 2 highly related conjugative plasmids, PL1 and PL3. Conjugative
181 plasmids typically have a limited number of plasmid copies (a maximum of 1 to 3 per
182 cell, maximum 10) (25). In fact, there is an incompatibility phenomenon between
183 replicons: the failure of 2 highly similar co-resident plasmids to be jointly inherited in a
184 stable manner. This failure is due to the plasmids' competition for replication factors or
185 to delayed plasmid replication after the plasmid segregation in daughter cells (26,27).
186 We examined the effect of cells tolerating only 1 plasmid copy (PL1 or PL3), where any
187 new incoming plasmid copy (either PL1 or PL3) is rejected or substituted by one of the
188 resident copies. We also examined the condition where only 2 plasmid copies can
189 coexist (2 PL1s or 2 PL3s; or 2 PL1 and 2 PL3) and when 3 plasmid copies can coexist
190 (all 3 PL1 or PL3; or 2 PL1 plus 1 PL3; or 2 PL3 plus 1 PL1). The question is
191 particularly relevant, given that the presence of plasmid PL1 (AbAR) (originally located
192 in *E. coli*) might prevent or influence the acquisition of plasmid PL3 (originally located
193 in *K. pneumoniae*) or vice versa. **Figure 2** shows the results of the effects of these
194 maximum plasmid copy numbers in the population structure of *E. coli* in the hospital
195 setting.

196

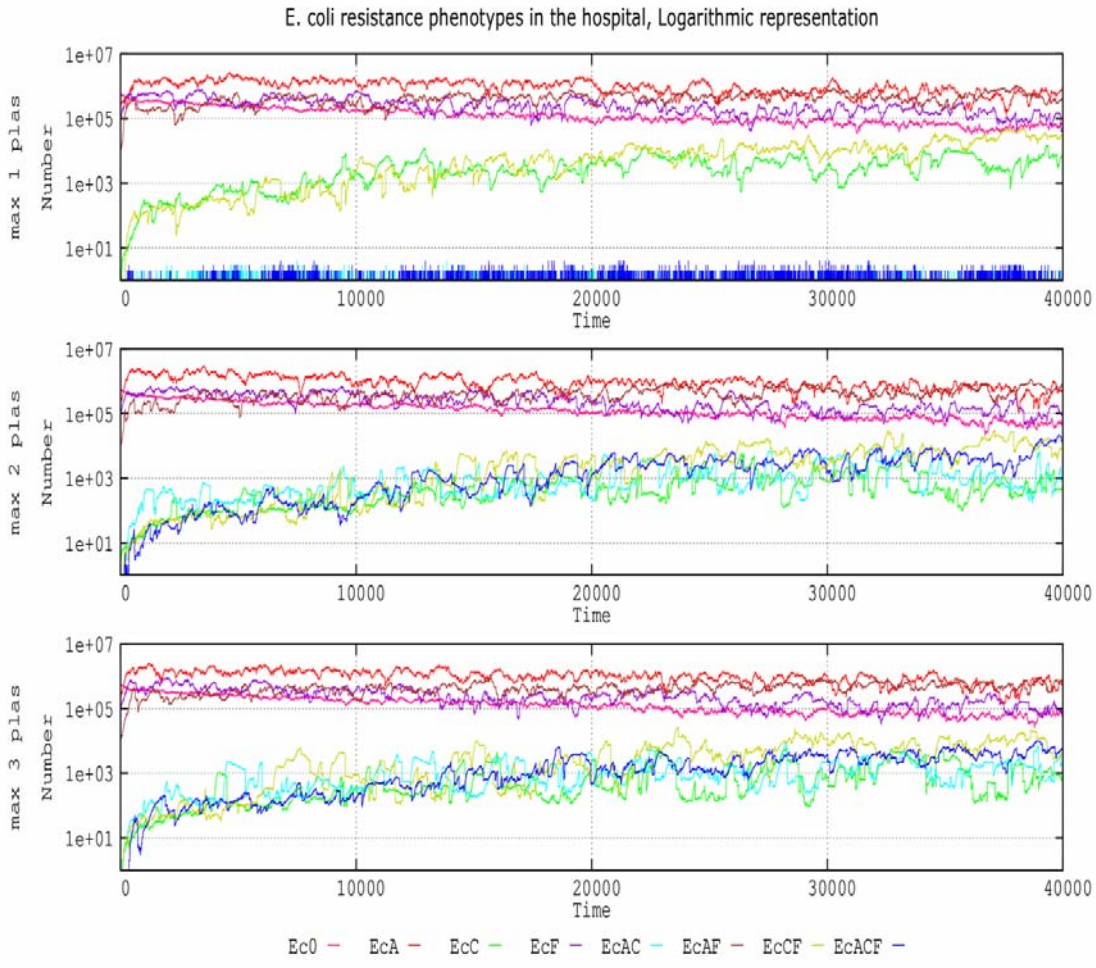

Figure 2. *Effect of plasmid incompatibility on the evolution of E. coli antibiotic resistance phenotypes in the hospital setting. Ec0, susceptible, no resistance plasmids (pink line), EcA, PL-AbAR (red); EcC, PL3-AbAR-AbCR (light fluorescent green), EcF, AbFR (violet) , EcAC, PL1-AbAR plus PL3-AbAR-AbCR, (light blue), EcAF, PL1-AbAR plus AbFR (brown), EcCF, PL3, AbAR-AbCR plus AbFR (olive green), EcACF, PL1-AbAR plus PL3-AbAR-AbCR plus AbFR (dark blue). The rate of plasmid cost compensation was fixed at 10-5. Numbers in ordinates are expressed in hecto-cells (one unit=100 cells in the microbiota)*

When a single copy of the plasmid replicon is tolerated in the cell (originally the plasmid-bearing *E. coli* cells have a copy of PL1), there is a progressive invasion of E. coli cells by the plasmid PL3 from *K. pneumoniae*, giving rise to an increase in the cephalosporin-resistant (and ampicillin-resistant) phenotype EcC (green line). Through mutation of these cells, the phenotype also includes the fluoroquinolone-resistant phenotype (olive green), which can also arise with even higher frequency by the acquisition of PL1 by AbFR cells and then by displacement of PL1 by PL3 (initially in *K. pneumoniae*). These cells lose PL1 (AbAR); even if the PL1 plasmid is transferred, it does not remain in the cell (blue spikes at the bottom curve). With a maximum of 2 or 3 plasmid copies per cell, we can obtain a similar increase in resistant populations harboring both PL1 and PL3, with or without fluoroquinolone resistance (dark and light blue, respectively).

Influence of random plasmid loss.

In the process of cell division, the daughter cell receives at least one plasmid as a result of random diffusion influenced by multimer resolution systems (28). In our model, plasmid loss produced plasmid-free cells. The rate of spontaneous plasmid loss remains controversial (29). Our results (Fig. 3) indicate that at loss (random segregation) rates of 10^{-3}, *E. coli* populations with plasmid PL1 or PL3 are not maintained beyond 8000 steps (approximately 2 weeks). At segregation rates of 10^{-4}, the most abundant plasmids (PL1 in *E. coli*, with AbAR, in red) are maintained. After an initial increase, however, the plasmid population containing PL3 steadily decreases because of the incompatibility of PL3 with the dominant PL1 and due to the progressive reduction of *K. pneumoniae* with PL3, reducing the flow toward *E. coli*. Of course, cells with PL3 are more effectively

selected than those with PL1, but PL1 is comparatively more abundant than PL3 in the ecosystem; therefore, PL1 is maintained along the 40,000 steps.

E. coli cells containing plasmid PL3 can slowly increase in number only at 10^{-5} segregation rates. At 10^{-6}, these cells reach the density of antibiotic-susceptible or PL1 - containing cells. These results suggest that, at high plasmid segregation rates, the populations harboring the most abundant plasmids in the ecosystem have an advantage over populations with minority plasmids; however, if the loss of plasmids is relatively rare (such as 10^{-6}), different plasmids might coexist in the population. Results with a 10^{-7} plasmid loss did not significantly differ from those of 10^{-6} (data not shown).

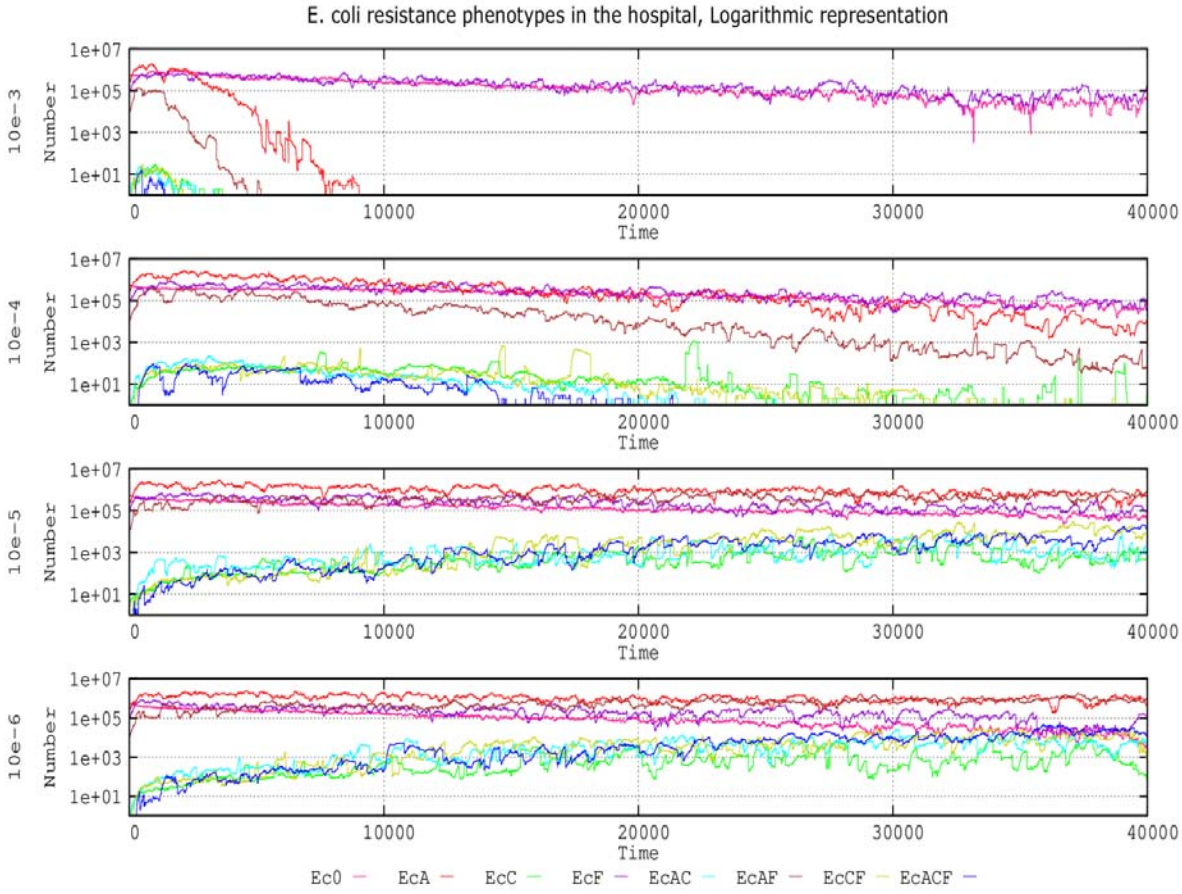

Figure 3. *Influence of plasmid loss rates on the evolution of E. coli resistance phenotypes in the*

hospital environment. Ec0, susceptible, no resistance plasmids (pink line), EcA, PL1-AbAR (red); EcC, PL3-AbAR-AbCR (light fluorescent green), EcF, AbFR (violet) , EcAC, PL1-AbAR plus PL3-AbAR-AbCR, (light blue), EcAF, PL1-AbAR plus AbFR (brown), EcCF, PL3, AbAR-AbCR plus AbFR (olive green), EcACF, PL1-AbAR plus PL3-AbAR-AbCR plus AbFR (dark blue). Compensation rate for plasmid fitness costs was fixed ad 10E-5. Numbers are expressed in hecto-cells (one unit=100 cells in the microbiota)

Influence of plasmid fitness costs

Plasmid fitness costs imposed to the bacterial host are considered a factor that contribute for the spreading success of a particular plasmid and their genes (30-33). Several values for PL1 and PL3 plasmid fitness costs were included in the model to ascertain the effect of hosting these plasmids (or not) on antibiotic resistance and species composition. For reference, a plasmid fitness cost of 0.06 indicates a 6% reduced growth rate for the *E. coli* and *K. pneumoniae* strains harboring the PL1 or PL3 plasmid). We investigated the influence of these values with "no fitness cost" (fitness cost = 0). Default values included in this model were as follows: only 2 plasmids can coexist in a single cell; the rate of spontaneous plasmid loss is 10^{-5}; the mutation rate to reduce 50% of the plasmid fitness cost is 10^{-8}. The results are presented in Figure 4.

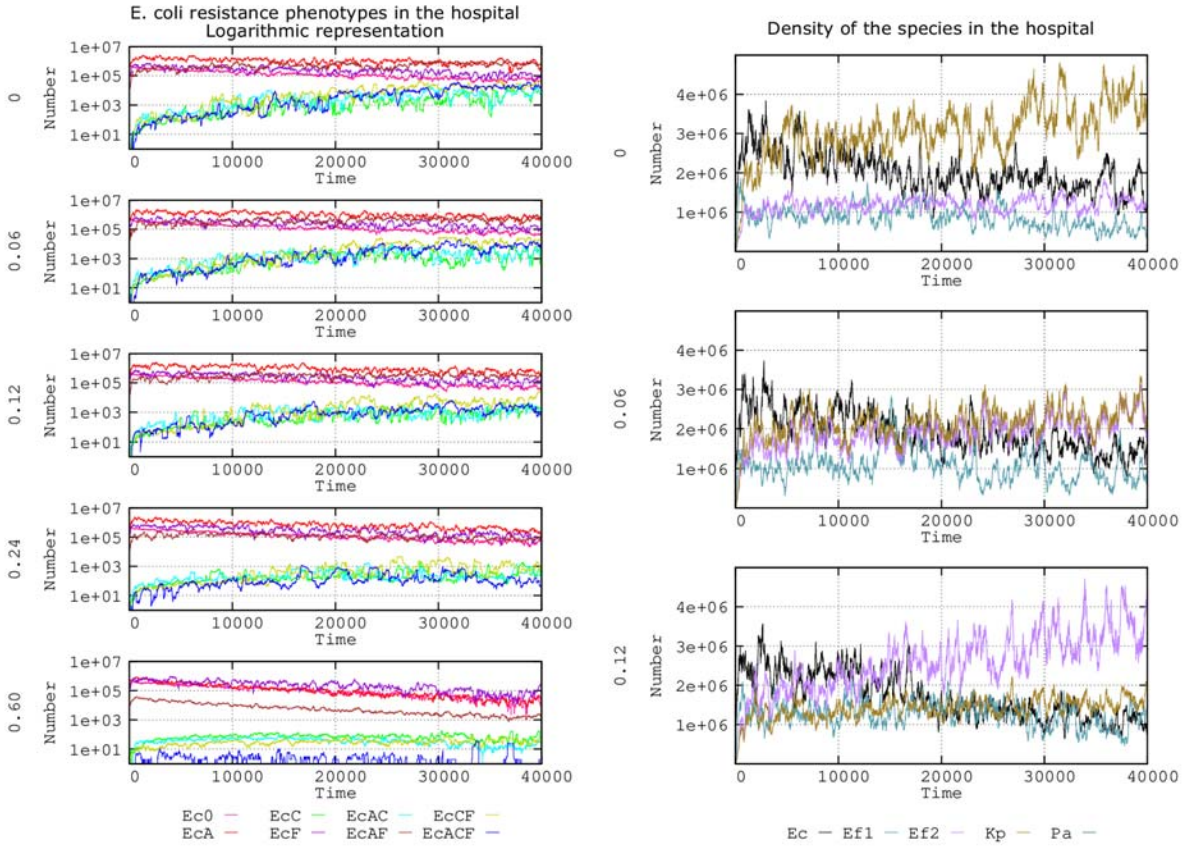

263

264 ***Figure 4.*** *Influence of plasmid fitness cost on the evolution of E. coli antibiotic resistance*
265 *phenotypes. The graphs in the left column show the effects for each fitness cost (0, 0.06, 0.12,*
266 *0.24, and 0.60). The lines indicate the following: Ec0, susceptible, no resistance plasmids (pink*
267 *line), On the left part, effects of no fitness cost (0), and 0.06, 0.12, 0.24, and 0.6 fitness costs.*
268 *Ec0, susceptible, no resistance plasmids (pink line), EcA, PL1-AbAR (red); EcC, PL3-AbAR-*
269 *AbCR (light fluorescent green), EcF, AbFR (violet) , EcAC, PL1-AbAR plus PL3-AbAR-AbCR,*
270 *(light blue), EcAF, PL1-AbAR plus AbFR (brown), EcCF, PL3, AbAR-AbCR plus AbFR (olive*
271 *green), EcACF, PL1-AbAR plus PL3-AbAR-AbCR plus AbFR (dark blue). The graphs in the*
272 *right column show the influence of 3 fitness costs (0.0, 0.06, 0.12) on the species distribution in*
273 *the simulated ecosystem: E. coli (black line), K. pneumoniae (olive green), ampicillin-R E.*
274 *faecium (violet), ampicillin-S E. faecium (blue-green). Numbers in ordinates are expressed in*
275 *hecto-cells (one unit=100 cells in the microbiota)*

Regarding *E. coli* phenotypes (Fig. 4, left column) the effect of increasing the plasmid fitness cost was to steadily reduce the number of strains harboring only PL3 (encoding AbCR) or PL3 and PL1, alone or in combination with PL1 (AbAR) or AbFR (green, blue, olive green, dark blue lines). Only with a high plasmid fitness cost (0.60) was there a clear reduction of the predominant populations containing PL1 in the absence (red line) or presence (brown line) of chromosomal AbFR, probably due to the maintenance of an effective plasmid transfer. Note that the population with only chromosomal mutation (not influenced by plasmid fitness cost [AbFR] rises to dominance (violet line) but tends to decrease slightly, possibly because the reduction in cell multiplication provides reduced cell densities and therefore encourages the emergence of an AbFR mutation.

Differences in plasmid costs, even comparing no cost with 0.06 or 0.12 plasmid costs, might influence the species structure in the hospital ecosystem. At cost 0, *K. pneumoniae* with PL3 (olive green) steadily increases in frequency. *K. pneumoniae* originally benefits from the AbAR (including AbA*R) and AbCR phenotype and progressively acquires fluoroquinolone resistance, surpassing *E. coli* with PL1, with only the AbAR phenotype (black). At cost 0.06, the long-term dominance of *K. pneumoniae* is strongly reduced, but *E. coli* also decreases in frequency. With a cost of 0.12, *E. faecium* (in which PL1 or and PL3 are naturally absent but with a AbAR-AbCR phenotype [due to AbAR and AbCR chromosomal PBPs, violet]) tends to dominate. Thus, the cost of harboring a plasmid (decreasing growth rates) might influence the abundance and diversity of species present in a particular environments.

Effect of changes in mutation frequency for compensation of plasmid fitness costs.

Mutation frequency should influence the emergence of plasmid cost compensatory mutations. Compensatory mutations in the bacterial chromosome (30,34) and in the

301 plasmid (35-38) might reduce the fitness cost of plasmid carriage, thus increasing the
302 replication rate of the hosting microorganisms and the spread of plasmids. The
303 emergence of compensatory mutations is certainly driven by the bacterial mutation
304 frequency, but the effect of mutation might be asymmetrical if it occurs in the
305 chromosome or plasmid, given that mutated plasmids can horizontally disseminate more
306 effectively than mutated chromosomes through vertical transmission and given the
307 presence of several genes that can compensate the cost, which differ among bacterial
308 hosts (3, 36-43). In our basic model, high overall mutation were expected to influence
309 not only plasmid cost compensation but also the selection of chromosomal mutants (for
310 instance, fluoroquinolone-resistant mutants). To separate the two effects in our model
311 and to detect the effect of compensating for plasmid fitness cost, we increased the
312 mutation frequencies but maintained the basic mutation frequency (10^{-8}) for AbFR
313 observed for rifampicin (44) that can be applied for AbFR (45). In this model, fitness
314 cost was established at 0.06, and the acquisition of a mutation reduces the fitness cost
315 by a default value of 0.5. At a normal mutation frequency (10^{-8}) or even 10^{-5} (data not
316 shown), the effect of different strengths of mutational compensation on the frequency of
317 plasmid-mediated antibiotic resistance was almost negligible in our model (**Fig. 5**).
318

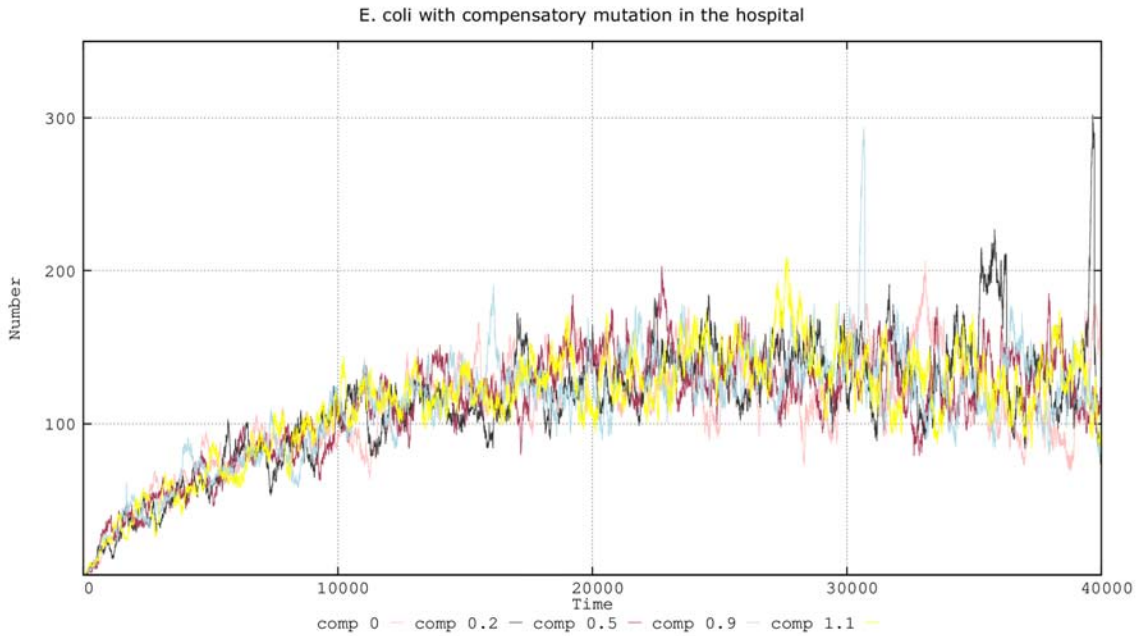

Figure 5*. Effect of different compensation strengths of plasmid fitness cost. Lines: 0, no compensation, pink; 0.2 cost compensation, black; 0.5 cost compensation, brown; 0.9 cost compensation, blue; 1.1 cost compensation, yellow. Numbers in ordinates are expressed in hecto-cells (one unit=100 cells in the microbiota)*

Figure 6 shows (left column) the effect of the 10-5 mutation frequency, which occurs by a small increase in *E. coli* lineages harboring compensated plasmids (olive green and dark blue lines), which is even more patent at the 10-3 mutation frequency. The reason for this small effect on *E. coli* can be explained by observing the overall landscape of the bacterial species included in the model (Fig. 6, right column); the proportion of compensated-plasmid-containing *K. pneumoniae* increases with the mutation frequency, probably at the expense of *E. coli* and *E. faecium*. Note that high mutation rates allow bacteria with initially low population sizes to cross the mutational threshold to obtain a beneficial mutation (46).

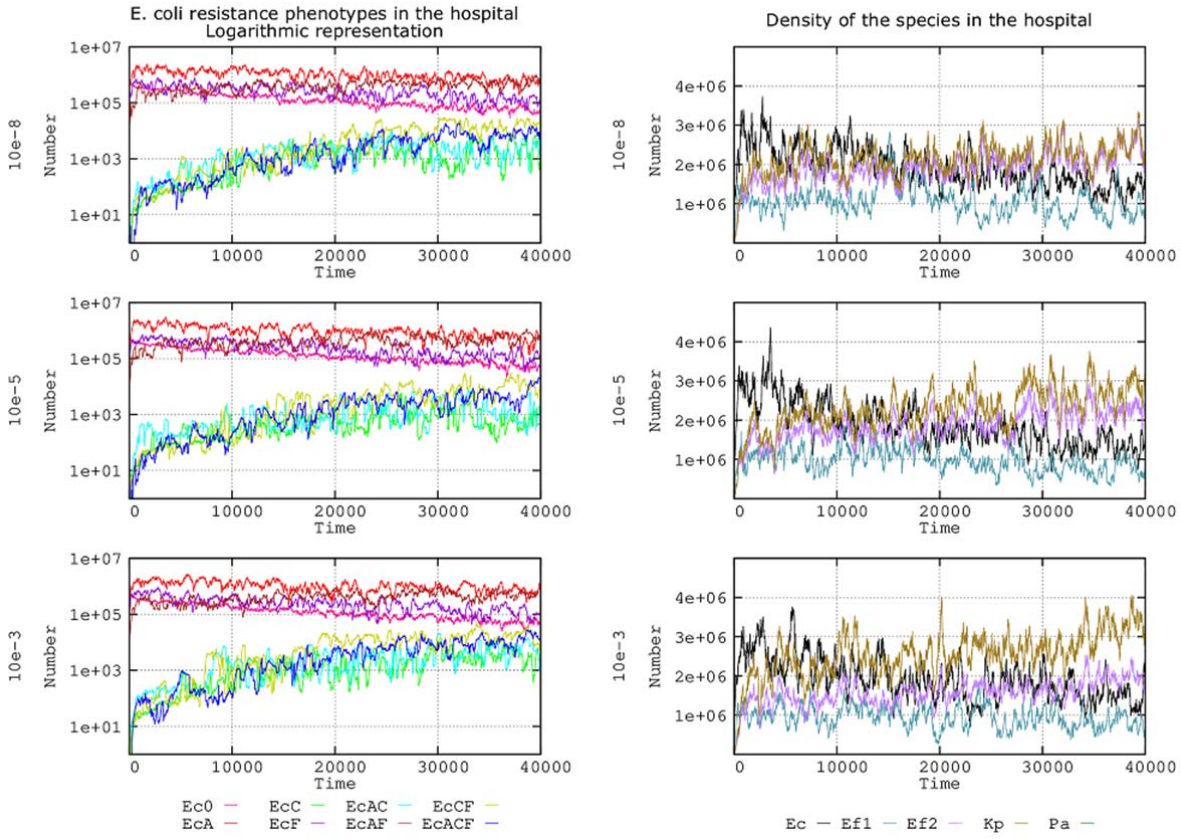

Figure 6. *The left column shows the influence of different mutation frequencies (10^{-8}, 10^{-5}, and 10^{-3}) compensating plasmid fitness costs in the evolution of E. coli resistance phenotypes. Ec0, susceptible to no resistance plasmids (pink line), EcA, PL1-AbAR (red); EcC, PL3-AbAR-AbCR (light fluorescent green), EcF, AbFR (violet) , EcAC, PL1-AbAR plus PL3-AbAR-AbCR, (light blue), EcAF, PL1-AbAR plus AbFR (brown), EcCF, PL3, AbAR-AbCR plus AbFR (olive green), EcACF, PL1-AbAR plus PL3-AbAR-AbCR plus AbFR (dark blue). The right column shows the corresponding effect on the species composition, E. coli (black line), K. pneumoniae (olive green), E. faecium ampicillin-R (violet), ampicillin-S E. faecium (blue-green). Numbers in ordinates are expressed in hecto-cells (one unit=100 cells in the microbiota)*

346 **Effect of changes in mutation frequency on combined fitness: compensation of**
347 **plasmid fitness costs and acquisition of fluoroquinolone resistance.**

348 In the natural world, we can consider that different mutation rates might influence
349 various bacterial functions differently. For instance, fluoroquinolone resistance
350 mutations in topoisomerases typically occur at a rate of 10^{-8}, but the frequency of
351 mutations influencing reductions in plasmid fitness costs might be much higher (e.g.,
352 10^{-5}) (40). In the Figure 7 there is a representation of the evolution in our complex
353 landscape of the number of cells with plasmid cost compensation with 10^{-8} or 10^{-5}
354 fluoroquinolone resistance mutation frequency.

355 Statistically, cells with emerging mutations resulting in AbFR rarely compensate the
356 plasmid costs; however, once an AbFR mutation selects an abundant resistant
357 population (47), there is a higher probability that a mutation will emerge in this
358 population and reduce the plasmid fitness cost. Figure 7 (up, left clumn) shows the
359 evolution of the number of cells in our complex landscape with plasmid cost
360 compensation when the mutation frequency for fluoroquinolone resistance was 10^{-8} or
361 10^{-5}. This result indicates that (as stated above), *regardless* of the mutational frequency
362 for plasmid cost compensation, the increased survival of fluoroquinolone-resistant cells
363 in the hospital environment increases the absolute number of plasmid cost
364 compensatory mutants. In the 2 panels of the first column of Figure 7b this effect is
365 visible in the higher nosocomial prevalence of *E. coli* (black line) when AbFR emerges
366 at a frequency of 10^{-5}. This strong increase in the AbA-AbFR population carrying PL1
367 (AbA) in *E. coli* (brown line) when the mutation frequency is 10^{-5} is depicted in Figures
368 7 (left column). The increase in cost-compensatory mutations of PL1 in the increased
369 AbA-AbFR population likely promotes its spread at these mutation frequencies,

competing with the less frequent plasmid (PL3), resulting in no clear advantage for AbCR (data not shown, available on request).

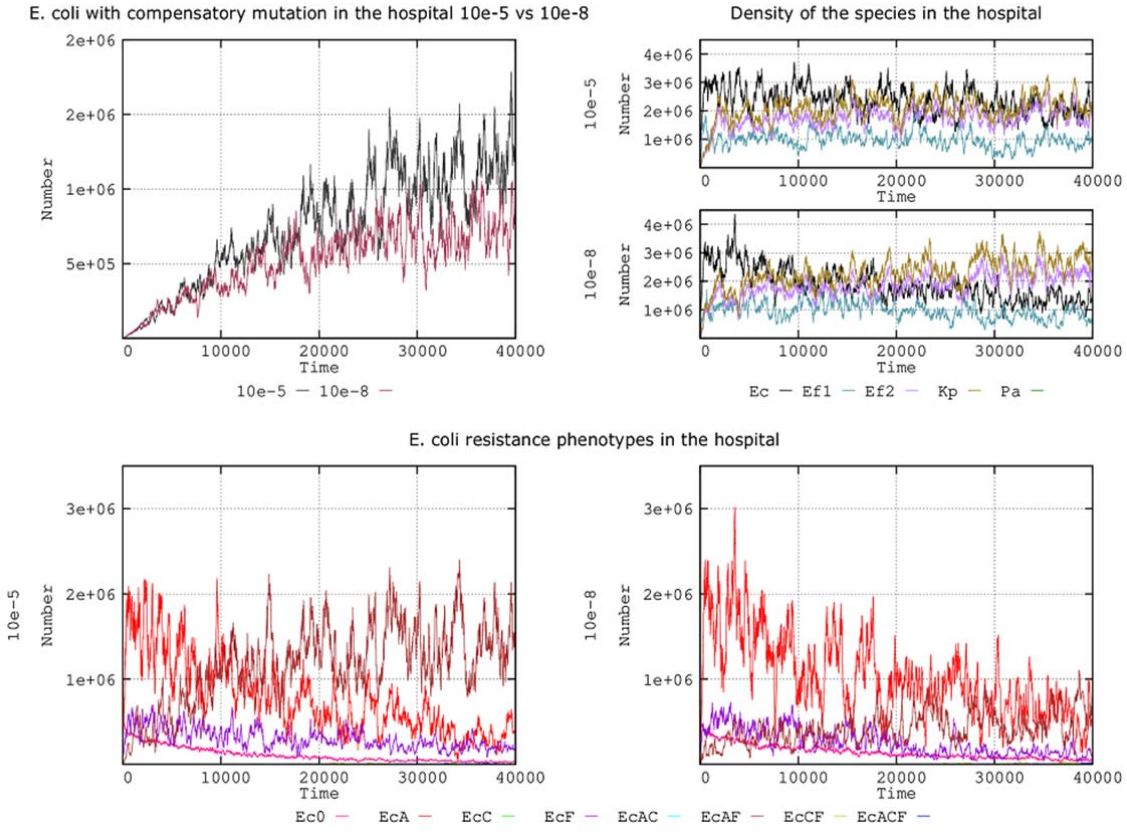

Figure 7*. Compensation of plasmid fitness costs and frequency for fluoroquinolone mutation. Upper left: E. coli cells compensated for fitness costs when mutation rates for fluoroquinolone resistance are 10^{-8} (black) or 10^{-5} (brown-violet). Upper right: the effect of these mutation rates on species distribution (E. coli [black line], K. pneumoniae [olive green], ampicillin-R E. faecium [violet], ampicillin-S E. faecium [blue-green]. Bottom: evolution of E. coli antibiotic resistance phenotypes at fluoroquinolone mutation frequencies of 10^{-5} (left) and 10^{-8} (right). Numbers are expressed in hecto-cells (one unit=100 cells in the microbiota)*

383

384 **Combined effects of compensation values for plasmid fitness cost and variation in**
385 **plasmid fitness cost**

386 Figure 8, left column (experiment with fixed mutation frequency for plasmid fitness
387 cost compensation of 10^{-5}) shows that the number of plasmid cost-compensated *E. coli*
388 is lower when the cost of carrying the plasmid increases (given that bacteria replicate
389 more slowly); however, cost-compensated bacteria (green line) outpace the non-
390 compensated bacteria (red line) much earlier. Thus, the expected benefit of mutational
391 compensation is proportional to the fitness cost imposed by the plasmid (37). By
392 increasing the plasmid fitness cost, the replication of bacteria is impaired, thus possibly
393 reducing the population size and the possibility of obtaining compensatory mutations.
394 Consequently, the reduction in plasmid fitness cost by compensatory mutations should
395 increase population sizes. On the other hand, the benefit of high mutation frequencies in
396 reducing the plasmid fitness cost should be proportional to this cost. Figure 8 (right
397 column) shows the outcome for our "hospital scenario" of the *E. coli* population with a
398 cost-compensated and a noncompensated plasmidome. For the same level of
399 compensation (0.2), the rise in compensated cells (green line) is higher for 0.12 than for
400 0.06 plasmid fitness costs. If we increase the fitness cost compensation level (to 0.5),
401 the rise in mutated cells is even higher, as expected, because the mutational yield is
402 proportional to the population size.

403

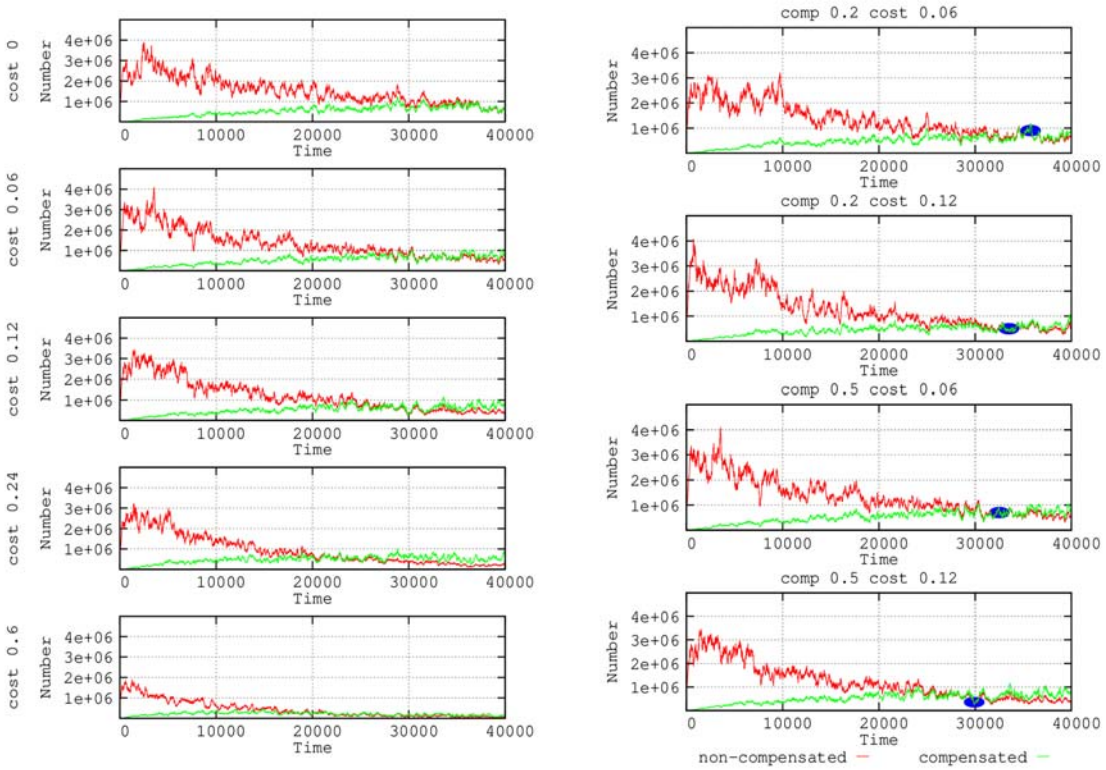

404

405

406

407 **Figure 8.** *Effects of plasmid compensation depending on the plasmid fitness cost. In the left*
408 *column, no compensated E. coli cells for plasmid fitness cost (green line) versus compensated*
409 *cells (red). In the right column, combinations of 2 fitness cost values (0.06 and 0.12) with 2*
410 *strengths of compensation values (0.2 and 0.5). Small blue ovals highlight that when the*
411 *plasmid cost is higher the compensation is more effective. Numbers in ordinates are expressed*
412 *in hecto-cells (one unit=100 cells in the microbiota)*

413 # Discussion

414 Plasmid biology should consider the multi-dimensional space where plasmids replicate
415 and disseminate, not only inside and between bacterial cells, but in complex ecosystems.

The application of membrane computing models to study the horizontal conjugative transfer of antibiotic resistance genes in bacteria (ref) is one of the few available approaches for addressing bacterial evolutionary dynamics in such a broad ecological context (14). Based on our previously published model (12), in this study the influence of various plasmid kinetic values in the evolution of antimicrobial resistance (8), was modeled within a complex system resembling the natural conditions that influence transmission at different levels (e.g., the flow of human hosts in the hospital and community, bacterial transmission/transfer rates among hosts, bacterial population sizes in the hosts, exposure and effects of various antibiotics in reducing bacterial numbers, selection of antibiotic resistant species, and the influence of "space for colonization" of resistant strains in the microbiota (12).

Details of the basic model's design have been presented elsewhere (11, 12, 13). These integrative models are mostly fed with data on plasmid biology obtained through *in-vitro* experiments and suggest that predictions based only on laboratory data might not necessarily reflect the evolution of resistance in natural clinical landscapes. This study presents only a model under particular conditions (see Materials and Methods section), which were selected as representative examples; however, many other conditions can be introduced into the parameters in our accessible model (https://sourceforge.net/projects/ares-simulator/). Our main findings might help explain the relative weight of parameters that modify plasmid kinetics in the evolution of antibiotic resistance.

Plasmid transmission rates (the conjugation rates in our model) have been considered one of the main drivers of the spread of antibiotic resistance genes in natural bacterial populations (27). In fact, there is a line of research on ecology-evolution (eco-evo) drugs that seeks to develop plasmid conjugation inhibitors to reduce the burden of

antibiotic resistance (48, 49). In our complex multilevel system and under the fixed conditions of the simulation, only high (10^{-3}) conjugation rates clearly influence the dissemination of plasmids and the resistances they contain. However, we were able to differentiate between conjugation rates of 10^{-6} (in which the plasmid PL3 slowly propagates) from 10^{-9} (in which effects or transfers are no longer visible). Interestingly, higher conjugation rates (at which *E. coli* transfer PL1 [AbAR] effectively) tend to displace PL3 (AbCR, AbAR) resistance in *K. pneumoniae* (through *par* incompatibility). Thus, the PL3 is only preserved under low conjugation rate conditions in *K. pneumoniae.*

Plasmid incompatibility refers to the number of plasmids (replicons) sharing the same *par* system (in our case, PL1 and PL3) that can coexist in the same cell. In our simulation and under conditions allowing only a single plasmid to be maintained, PL3 (containing AbCR-AbAR) from *K. pneumoniae* can displace PL1 (AbAR); thus, AbCR significantly increases in *E. coli*. Conversely, the introduction of PL1 from *E. coli* into *K. pneumoniae* severely reduces the number of *K. pneumoniae* cells harboring PL3. In the conditions set in the present simulation (conjugation rate 10^{-6}), if the cell tolerates 2 replicon copies and PL1 + PL3 can coexist, the number of *E. coli* cells harboring PL3 (AbCR) comparatively decreases, and there are no significant differences if the cell is able to maintain 3 replicons, a result that might be modified by the conjugation rate. In a previous published study by our group (12), *K. pneumoniae* retained PL3 (AbCR) if the conjugation rate is higher, 10E-4. Note that in the real world, *K. pneumoniae* frequently serves to introduce in the ecosystem plasmids with AbCR, that are then transferred to *E. coli*, and subsequently among *E. coli* populations (50, 51). Because *E. coli* has a comparatively higher population size, and most of the conjugations occur at the intraspecies level, in many cases the AbCR hospital “epidemics” tends to occur at long

466 term in *E. coli*, and AbCR *K. pneumoniae* is usually maintained at a lower frequency
467 (52,53,54,55).

468 Plasmids segregate (disappear, are lost) from the cells in which they are hosted, but the
469 segregation rates are not well established and depend on the ecological-physiological
470 conditions of the bacteria and the segregation mechanisms. In our model system,
471 plasmid loss rates of 10^{-3} led to plasmid extinction. In general, high segregation rates
472 favor plasmids contained in large bacterial populations. At 10^{-4}, for example, only PL1,
473 contained in the dominant *E. coli* population persists in time, displacing populations
474 with PL3, despite the stronger selection pressure (due to AbCR). Higher exposure to
475 antibiotics (cephalosporins) selecting for PL3 should logically favor the maintenance of
476 PL3. In any case, PL3 persists much more effectively at low segregation levels (such as
477 10^{-5} and 10^{-6}).

478 Plasmids fitness costs, expressed as a reduction in bacterial growth rate, has a relevant
479 influence on bacterial resistance phenotypes, particularly on the propagation of plasmids
480 hosted by minority populations. This effect is particularly visible when the plasmid cost
481 is $\geq$0.12. For instance, the spread of PL3 (with AbCR) primarily hosted by *K.*
482 *pneumoniae* is strongly reduced beyond a cost of 0.12. Even if the same cost was
483 imposed by PL1, as is frequently present in the dominant *E. coli*, the reduction in fitness
484 is somewhat compensated by intra-specific transfer; however, when the fitness costs is
485 0.60, the population with PL1 steadily decreases. Although AbFR populations are not
486 influenced by plasmid fitness costs, many of the AbFR cells are lost because of the
487 reduced reproductive rate imposed by the cost of plasmid they might contain.

488 Mutations might compensate the plasmid fitness costs. The mutation frequency should
489 therefore affect the number of cost-compensated plasmids, particularly of the plasmids
490 imposing a higher fitness cost. In our model, the effect on plasmid-mediated resistance

was almost undetectable at the "consensus" mutation frequency (10^{-8}), which might suggest that this compensation parameter has low epidemiological consequences. Even at a general mutation frequency of 10^{-5}, the effects on the spread of antibiotic resistance under our experimental conditions were barely detectable. Of course, there are hypermutable strains (with a 10^{-6} or 10^{-5} mutation rate), and considering that the frequency of mutations influencing plasmid compensation might reach 10^{-5} (40), we cannot reject the possibility of scenarios in which the mutational cost compensation of *E. coli* lineages harboring compensated plasmids tends to increase (56). In fact, this might explain why *E. coli* isolates harboring plasmids with extended-spectrum β-lactamases have increased mutation frequencies (57). As proof of this concept, the benefit for cost-compensated strains (and for *K. pneumoniae*) becomes clear in a hypothetical scenario containing strains with a 10^{-3} mutation frequency (37).

Given that increases in general mutation frequency should necessarily influence the emergence of chromosomal fluoroquinolone-resistance mutations (AbFR), we combined the effects of the mutation rate on AbFR acquisition and plasmid-cost compensatory mutation. Our results indicate that, regardless of the mutational frequency for plasmid cost compensation, the increased survival and population increase of fluoroquinolone-resistant cells with high mutation rates increase the absolute number of plasmid-cost compensatory mutants.

In principle, the beneficial effect of plasmid cost compensation on the evolution of plasmid spread should be proportional to the reduction in fitness imposed by plasmid carriage. On one hand, our simulation shows that the cost-compensated bacteria surpass the number of non-compensated bacteria earlier when the cost is high. However, the number of plasmid cost-compensated *E. coli* decreases when the cost of carrying the

515 plasmid increases, given that the availability of mutants is dependent on the population
516 size.

517 Note that the results of this study correspond to a limited number of possible parametric
518 landscapes; however, our intention was to use the parameters that frequently influence
519 plasmid and bacterial dissemination in hospital settings. In any case, a major advantage
520 of the membrane computing modeling technology is its *scalability*, allowing to include
521 many different parametric values simultaneously in the model at the various hierarchical
522 levels considered in particular ecosystems in workload and scope. How changes in a
523 "piece" (the plasmid) contributes to create a particular "pattern" in a nested system of
524 biological units, expanding from the genes and cells to the communities of human hosts
525 and environments, is certainly one of the challenges of modern research on antibiotic
526 resistance (6, 58, 59).

527

528 # Materials and Methods

529 **Computing model**.

530 All computational simulations were performed using an updated version of the
531 Antibiotic Resistance Evolution Simulator (ARES), which is a P system software
532 implementation for modeling antibiotic resistance evolution (11, 13). The current
533 version of ARES (2.0) can be freely downloaded at https://sourceforge.net/projects/ares-
534 simulator/. The original ARES website http://gydb.uv.es/ares, offers information on the
535 rules and parameters currently used by ARES and facilitates customer generation of
536 specific scenarios to model the evolution of antibiotic resistance.

537 **The basic model application: quantitative structure.**

538 A detailed account of the main features of our model's quantitative structure is available
539 in our previous publication (12), a summary of which is presented below.

540 **Hospitalized hosts, admissions, and discharge rates in the population**. The number
541 of hosts in the hospital reflects an optimal proportion of 10 hospital beds per 1000
542 individuals in the community (https://data.oecd.org/healtheqt/hospital-beds.htm). The
543 hospital has 100 occupied beds and corresponds to a population of 10,000 individuals in
544 the community. The admission and discharge rates from hospital are equivalent to 3–10
545 individuals/10,000 population/day (http://www.cdc.gov/nchs/data/nhds/1general/). In
546 the basic model, 6 individuals from the community are admitted to the hospital and 6
547 are discharged from the hospital to the community per day (approximately at 4 hour-
548 intervals). Approximately 75% of the patients stay in the hospital between 6 and 9 days.

549 **Transfer of bacterial organisms between hospitalized hosts**. We used a "contagion
550 index" of 5% (for every 100 hospitalized patients, 5 "donors" transmit bacteria to
551 another 5 "recipients" per hour. Bacterial transmission includes the spread of normal
552 microbiota. The hospital is surrounded by a community of healthy individuals,
553 occasionally admitted to the hospital, with a "contagion index" of 0.01%.

554 **Exposure to antibiotic agents.** We considered 3 types of commonly used antibiotics to
555 be employed during a 7-day treatment: aminopenicillins (AbA), third-generation
556 cephalosporins, as cefotaxime (AbC), and fluoroquinolones (AbF). In the basic model,
557 20% of the individuals in the hospital compartment are under antibiotic exposure each
558 day. Antibiotics AbA-AbC-AbF are employed in the hospital at a proportion
559 (percentage) of 30-40-30, respectively. A single patient is treated with only one
560 antibiotic, administered every 8 hours. After each dose is administered, all 3
561 (bactericidal) antibiotics induce after a decrease of 30% in the susceptible population
562 after the first hour of dose exposure, and a 15% reduction in the second hour. In the

563 community surrounding the hospital, 1.3% of individuals are undergoing antibiotic
564 therapy; AbA-AbC-AbF is employed at a proportion of 75-5-20, respectively**.**

565 **The bacterial colonization space** of the populations of the considered clinical species
566 (*E. coli*, *K. pneumoniae*, *Pseudomonas aeruginosa*, *Enterococcus faecium*) and other
567 basic colonic microbiota populations is defined as the volume they occupy in the
568 intestine. In natural conditions, the sum of these populations is estimated at 10^8 cells per
569 mL of colonic content. Clinical species constitute only 1% of the cells in each mL and
570 have a basal colonization space of 1% of each mL of colonic content (or 0.01 mL).
571 Other microbiota populations are considered a single ensemble. The colonic space
572 occupied by these populations can change due to antibiotic exposure. AbA, AbC, and
573 AbF reduce the intestinal microbiota 25%, 20%, and 10%, respectively. This space can
574 be occupied by resistant populations of these human opportunistic pathogens; however,
575 in the absence of antibiotic exposure, the colonic populations tend to return to the basal
576 population size, which would occur in 2 months (60, 61).

577 **Populations' operative packages and counts.** To facilitate the execution of the model,
578 we considered that 10^8 cells in nature is equivalent to 10^6 cells in the model. In other
579 words, one "hecto-cell" (h-cell) in the model is an "operative package" of 100 cells in
580 the real world. Given the high effective population sizes in bacteria, these 100 cells are
581 considered a uniform population of a single cell type. For computational efficiency, we
582 considered that each patient (in the hospital) or individual (in the community) is
583 represented in the model by 1 mL of its colonized colonic space (approximately 3000
584 mL) and is referred to as a "host-mL". Our results as therefore represented as "number
585 of h-cells in all host-mLs" in most of the figures.

586 **Quantitative distribution of species and clones.** In the basal scenario, the species
587 distribution in these 1,000,000 cells (contained in 1 ml) was as follows: for *E. coli*,

860,000 cells, including 500,000 susceptible cells, 250,000 containing PL1-AbAR, 100,000 with the AbFR mutation, and 10,000 with the AbFR mutation and carrying PL1 (AbAR); for *E. faecium*, 99,500 cells susceptible to both AbA and AbF and 20,000 cells with chromosomal AbCR, AbFR, and CO1-AbAR (CO for *Enterococcus* conjugative element); for *K. pneumoniae*, 20,000 cells, with chromosomal AbAR and AbFR, also harboring PL3 (AbCR-AbAR); and *P. aeruginosa*, 500 cells containing PL3 (AbCR-AbAR) and chromosomal AbAR. At time 0, this distribution was identical in hospitalized and community patients.

Bacterial multiplication rates. We considered the basal multiplication rate (corresponding to *E. coli* 0) to be equal to 1, in which each bacterial cell gives rise to 2 daughter cells every hour. Comparatively, the rates for *E. faecium*, *K. pneumoniae*, and *P. aeruginosa* were 0.85, 0.9, and 0.15, respectively. In these basic conditions, the acquisition of a plasmid or other incurs an cost of 0.06, while the acquisition of the AbFR mutation incurs a cost of 0.01 (1% reduction in growth rate) The number of cell replications will be limited by the available space (see above).

Plasmids and antibiotic resistance types. For the sake of simplicity, this study considered 2 plasmids sharing the same partition system and therefore competing for replication when hosted in the same cell, with either 1) resistance to AbA, A for aminopenicillins) present in plasmid PL1, primarily hosted in *E. coli*, or (2) resistance to antibiotic C plus antibiotic A (AbC, C for third generation cephalosporins), primarily determined by the plasmid PL3, primarily hosted in *K. pneumoniae*. Note that some widely spread plasmids that encode extended-spectrum beta-lactamases (ESBLs) frequently carry genes for AbA resistance. In addition, mutational events lead to the emergence of chromosomal fluoroquinolone resistance (AbF, F for fluroquinolones). Organisms mutate to AbF at the same rate: 1 mutant for every 10^8 bacterial cells per cell

division. Note that *K. pneumoniae* has intrinsic (plasmid-independent) resistance to AbA. Although it was not analyzed in this study (but is included in the model), a clone of *E. faecium* resistant to AbA might transfer this resistance to a susceptible clone at a rate of 10^{-4} (62).

Basal plasmid kinetic values. We established a basal set of plasmid kinetic values, based on reports in the literature (1,2, 19-23). In the simulation, modifications to each value were applied, maintaining the other values fixed; ultimately, more than one parameter was modified to ascertain the combined effects. The applied basal plasmid kinetic values were as follows: a) a plasmid transfer rate of 10^{-6} per hour; i.e., 1 in 100,000 or 1 million donor-recipient contacts that result in random and reciprocal cell-to-cell *E. coli-K. pneumoniae* transfer of the plasmid (10^{-9} from each of them to *P. aeruginosa*) every hour; b) a plasmid incompatibility rate of 2 plasmids/cell, indicating that, in the presence of a third plasmid, one of the three is stochastically removed; c) a rate of plasmid cost of 0.06; i.e., the bacterial growth rate is decreased by 6% when harboring plasmids); d) a rate of frequency of mutational plasmid cost compensation of 10^{-5}; i.e., in 1 per 100,000 cells, a mutational event in the plasmid or bacterial genome decreases the plasmid cost by 50%; e) a rate of mutational events leading to significant fluoroquinolone resistance of 10^{-8}; and f) a rate of plasmid segregation of 10^{-5}, indicating that stochastically 1 cell among 100,000 eliminates the plasmid it contains.

Acknowledgements

F. Baquero, M. Campos, and T. M. Coque were supported by EU Joint Programming Initiative JPIAMR2016-AC16/00043 (JPIonAMR-Third call on Transmission, ST131TS project), the Health Institute Carlos III of Spain (grants PI15-00818 and PI18-01942 and CIBER (CIBER in Epidemiology and Public Health, CIBERESP;

637 CB06/02/0053)) and the Regional Government of Madrid (InGEMICS-C; S2017/BMD-
638 3691); all of them cofinanced by the European Development Regional Fund [ERDF] "A
639 Way to Achieve Europe". A. San Millan was supported by the European Research
640 Council under the European Union's Horizon 2020 Research and Innovation Program
641 (ERC grant agreement no.757440-PLASREVOLUTION).

642

643

644 **REFERENCES**

645 **1.** Stewart FM, Levin BR. 1977. The population biology of bacterial plasmids: a
646 priori conditions for the existence of conjugationally transmitted
647 Factors. Genetics 87:209–228.
648 **2.** Bergstrom CT, Lipsitch M, Levin BR. 2000. Natural selection, infectious transfer
649 and the existence conditions for bacterial plasmids. Genetics 155:1505-1519.
650 **3.** De Gelder L, Ponciano JM, Joyce P, Top EM. 2007. Stability of a promiscuous
651 plasmid in different hosts: no guarantee for a long-term relationship.
652 Microbiology 153:452–463.
653 **4.** Norman A., Hansen LH, Sørensen, SJ. 2009. Conjugative plasmids: vessels of
654 the communal gene pool. Phil Trans R Soc B: Biol Sci 364:2275-2289.
655 **5.** Andam CP, Fournier GP, Gogarten JP. 2011. Multilevel populations and the
656 evolution of antibiotic resistance through horizontal gene transfer. FEMS
657 Mmicrobiol Rev 35:756-767
658 **6.** Baquero F, Tedim ASP, Coque TM. 2013. Antibiotic resistance shaping multi-
659 level population biology of bacteria. Front Microbiol: 4, 15
660 **7.** Wein T, Hülter NF, Mizrahi I. Dagan T. 2019. Emergence of plasmid stability
661 under non-selective conditions maintains antibiotic resistance. Nat Commun
662 10:2595
663 **8.** Yano H, Shintani M, Tomita M, Suzuki H, Oshima T. 2019. Reconsidering
664 plasmid maintenance factors for computational plasmid design. Comp Struct
665 Biotech J 17:70-81.
666 **9.** Gumpert H, Kubicek-Sutherland JZ, Porse A, Karami N, Munck C, Linkevicius
667 M, Adlerberth I, Wold AE, Andersson DI, Sommer MOA. 2017. Transfer and

668 persistence of a multi-drug resistance plasmid in situ of the infant gut microbiota
669 in the absence of antibiotic treatment. Front Microbiol 8:1852.
670 **10.** Durão P, Balbontín R, Gordo I. 2018. Evolutionary mechanisms shaping the
671 maintenance of antibiotic resistance. Trends Microbiol, 26:677-691.
672 **11.** Campos M, Llorens C, Sempere JM, Futami R, Rodriguez I, Carrasco P, Futami
673 R, Rodriguez I, Capilla R, Latorre A, Coque TM, Moya A, Baquero F. 2015. A
674 membrane computing simulator of trans-hierarchical antibiotic resistance
675 evolution dynamics in nested ecological compartments (ARES). Biol direct,
676 10(1), 41
677 **12.** Campos M, Capilla R, Naya F, Futami R, Coque T, Moya A, Fernandez-Lanza V,
678 Cantón R, Sempere JM, Llorens C, Baquero F. 2019. Simulating multilevel
679 dynamics of antimicrobial resistance in a membrane computing model. mBio
680 10:e02460-18.
681 **13.** Baquero F, Campos,M, Llorens C, Sempere JM. 2018. A model of antibiotic
682 Resistance evolution dynamics through P systems with active membranes and
683 communication rules. In Enjoying natural computing. Graciani C, Agustín
684 Riscos-Núñez A, Păun Gh, Rozenberg G, Salomaa A (ed). p 33-44. Springer,
685 Cham.
686 **14.** Leclerc QJ, Lindsay JA, Knight GM. 2019. Mathematical modelling to study the
687 horizontal transfer of antimicrobial resistance genes in bacteria: current state of
688 the field and recommendations. J. R. Soc. Interface 16: 20190260
689 **15.** Blanquart F. 2019. Evolutionary epidemiology models to predict the dynamics of
690 antibiotic resistance. Evol Appl 12:365-383
691 **16.** Rozenberg G, Salomaa A, Păun G. (ed). 2010. The Oxford handbook of
692 membrane computing. Oxford University Press. Oxford.

693 **17.** Păun, Gh. 2002. Membrane Computing. An Introduction. Springer-Verlag,
694 Heidelberg
695 **18.** Simonsen L, Gordon DM, Stewart FM, Levin BR. 1990. Estimating the rate of
696 plasmid transfer: an end-point method. Microbiology, 136:2319-2325.
697 **19.** Levin BR, Stewart FM, Rice VA. 1979. The kinetics of conjugative plasmid
698 transmission: fit of a simple mass action model. Plasmid 2:247–260.
699 **20.** Dionisio F, Matic I, Radman M, Rodrigues OR, Taddei F. 2002. Plasmids spread
700 very fast in heterogeneous bacterial communities. Genetics 162: 1525-1532
701 **21.** Turner PE, Williams ESCP, Okeke C, Cooper VS, Duffy S, Wertz JE. 2014.
702 Antibiotic resistance correlates with transmission in plasmid evolution. Evolution
703 68:3368-3380.
704 **22.** Porse A, Schønning K, Munck C, Sommer MO. 2016. Survival and evolution of
705 a large multidrug resistance plasmid in new clinical bacterial hosts. Mol Biol
706 Evol 33:2860-2873.
707 **23.** Zhong X, Droesch J, Fox R, Top EM, Krone SM. 2012. On the meaning and
708 estimation of plasmid transfer rates for surface-associated and well-mixed
709 bacterial populations. J Theor Biol 294:144-152..
710 **24.** Hyland EM, Wallace EW, Murray AW. 2014. A model for the evolution of
711 biological specificity: a cross-reacting DNA-binding protein causes plasmid
712 incompatibility. J Bacteriol 196:3002-3011.
713 **25.** Paulsson J. 2002. Multilevel selection on plasmid replication. Genetics 161:
714 1373–1384.
715 **26.** Carattoli A. 2009. Resistance plasmid families in Enterobacteriaceae. Antimicrob
716 Agents Chemother 53:2227-2238.

717 **27.** Taylor DE, Gibreel A, Tracz DM, Lawley TD. 2004. Antibiotic resistance
718 plasmids. In Plasmid Biology, Funnell BE, Phillips GJ (ed) (pp. 473-492).
719 American Society of Microbiology.
720 **28.** Million-Weaver S, Camps M. 2014. Mechanisms of plasmid segregation: have
721 multicopy plasmids been overlooked? Plasmid 75:27-36.
722 **29.** Lau BT, Malkus P, Paulsson J. 2013. New quantitative methods for measuring
723 plasmid loss rates reveal unexpected stability. Plasmid 70:353-361.
724 **30.** Vogwill T, MacLean RC. 2015. The genetic basis of the fitness costs of
725 antimicrobial resistance: a meta-analysis approach. Evol Appl 8:284-295
726 **31.** Andersson DI., Levin BR. 1999. The biological cost of antibiotic resistance. Curr
727 Opin Microbiol 2: 489-493.
728 **32.** Haft R, Mittler J, Traxler B. 2009. Competition favours reduced cost of plasmids
729 to host bacteria. ISME J 3, 761–769
730 **33.** San Millán A, MacLean RC. 2017. Fitness costs of plasmids: a limit to plasmid
731 transmission. Microbiol Spectr 5:5
732 **34.** Andersson DI, Hughes D. 2010. Antibiotic resistance and its cost: is it possible to
733 reverse resistance? Nat Rev Microbiol 8:260-271.
734 **35.** Loftie-Eaton W, Bashford K, Quinn H, Dong K, Millstein J, Hunter S, Thomason
735 MK, Houra Merrikh H, Ponciano JM, Top EM. 2017. Compensatory mutations
736 improve general permissiveness to antibiotic resistance plasmids. Nat Ecol Evol
737 1:1354
738 **36.** Zwanzig M, Harrison E, Brockhurst MA, Hall JP, Berendonk TU, Berger U.
739 2019. Mobile compensatory mutations promote plasmid survival. mSystems
740 4:e00186-18

741 **37.** Yang QE, MacLean C, Papkou A, Pritchard M, Powell L, Thomas D, Andrey DO,
742 Li M, Spiller B, Yang W, Walsh TR. 2020. Compensatory mutations modulate
743 the competitiveness and dynamics of plasmid-mediated colistin resistance in
744 Escherichia coli clones. ISME J 14:861–865
745 **38.** Gama JA, Zilhão R, Dionisio F. 2018. Impact of plasmid interactions with the
746 chromosome and other plasmids on the spread of antibiotic resistance. Plasmid
747 99:82-88.
748 **39.** Harrison E, Guymer D, Spiers AJ, Paterson S, Brockhurst MA. 2015. Parallel
749 compensatory evolution stabilizes plasmids across the parasitism-mutualism
750 continuum. Curr Biol, 25:2034-2039
751 **40.** Harrison E, Dytham C, Hall JP, Guymer D, Spiers AJ, Paterson S, Brockhurst,
752 MA. 2016. Rapid compensatory evolution promotes the survival of conjugative
753 plasmids. Mob Genet Elements 6:2034-2039.
754 **41.** Hall JPJ, Brockhurst MA, Dytham C, Harrison E. 2017. The evolution of plasmid
755 stability: Are infectious transmission and compensatory evolution competing
756 evolutionary trajectories? Plasmid 91:90-95.
757 **42.** San Millan, A. Peña-Miller R, Toll-Riera M, Halbert ZV, McLean AR, Cooper
758 BS, MacLean RC. 2014 Positive selection and compensatory adaptation interact
759 to stabilize non-transmissible plasmids. Nat Commun 5: 5208 812
760 **43.** Shintani M., Suzuki H. 2019. Plasmids and Their Hosts. In: Nishida H., Oshima
761 T. (ed) DNA Traffic in the Environment. Springer, Singapore
762 **44.** Baquero MR, Nilsson AI, Turrientes C, Sandvang D, Galán JC, Martínez JL,
763 Frimodt-Møller N, Baquero F, Andersson DI. 2004. Polymorphic mutation
764 frequencies in Escherichia coli: emergence of weak mutators in clinical isolates. J
765 Bact 186:5538-5542.

766 **45.** Lindgren PK, Karlsson Å, Hughes D. 2003. Mutation rate and evolution of
767 fluoroquinolone resistance in Escherichia coli isolates from patients with urinary
768 tract infections. Antimicrob. Agents Chemother 47:3222-3232.
769 **46.** LeClerc JE, Li B, Payne W, and Cebula TA. 1996. High mutation frequencies
770 among Escherichia coli and Salmonella pathogens. Science 274:1208-1211
771 **47.** Redgrave LS, Sutton SB, Webber MA, Piddock LJ. 2014. Fluoroquinolone
772 resistance: mechanisms, impact on bacteria, and role in evolutionary success.
773 Trends Microbiol 22:438-445
774 **48.** Baquero F, Coque TM, De La Cruz F. 2011. Ecology and evolution as targets:
775 the need for novel eco-evo drugs and strategies to fight antibiotic resistance.
776 Antimicrob Agents Chemother 55:3649-3660.
777 **49.** Buckner MM, Ciusa ML, Piddock LJ. 2018. Strategies to combat antimicrobial
778 resistance: anti-plasmid and plasmid curing. FEMS Microbiol Rev 42:781-804
779 **50.** Bush K. 2008. Extended-spectrum β-lactamases in North America, 1987–2006.
780 Clin Microbiol Infect 14:134-143.
781 **51.** Jacoby GA, Han P. 1996. Detection of extended-spectrum beta-lactamases in
782 clinical isolates of *Klebsiella pneumoniae* and *Escherichia coli*. J Clin Microbiol
783 34:908-911.
784 **52.** Valverde A, Coque TM, Sánchez-Moreno MP, Rollán A, Baquero F, Cantón R.
785 2004. Dramatic increase in prevalence of fecal carriage of extended-spectrum β-
786 lactamase-producing Enterobacteriaceae during nonoutbreak situations in Spain.
787 J Clin Microbiol 42:4769-4775.
788 **53.** Hernández J R, Martínez-Martínez L, Cantón R, Coque TM, Pascual, A. 2005.
789 Nationwide study of *Escherichia coli* and *Klebsiella pneumoniae* producing

790 extended-spectrum β-lactamases in Spain. Antimicrob Agents Chemother 49:
791 2122-2125.
792 **54.** Perez F, Endimiani A, Hujer KM, Bonomo RA. 2007. The continuing challenge
793 of ESBLs. Curr Opin Pharmacol, 7:459-469.
794 **55.** Hernández-García M, Pérez-Viso B, Navarro-San Francisco C., Baquero F,
795 Morosini MI, Ruiz-Garbajosa P, Cantón R. 2019. Intestinal co-colonization with
796 different carbapenemase-producing Enterobacterales isolates is not a rare event in
797 an OXA-48 endemic area. EClinicalMedicine, 15:72-79.
798 **56.** McNally A, Oren Y, Kelly D, Pascoe B, Dunn S, Sreecharan T, Vehkala M,
799 Välimäki N, Prentice MB, Ashour A, Avram O, Pupko T, Dobrindt U, Literak I,
800 Guenther S, Schaufler K, Wieler LH, Zhiyong Z, Sheppard SK, McInerney JO,
801 Corander J. 2016. Combined analysis of variation in core, accessory and
802 regulatory genome regions provides a super-resolution view into the evolution of
803 bacterial populations. PLoS Gen, 12(9).
804 **57.** Baquero MR, Galán JC, Turrientes MC, Cantón R, Coque TM, Martínez JL,
805 Baquero, F. 2005. Increased mutation frequencies in *Escherichia coli* isolates
806 harboring extended-spectrum β-lactamases. Antimicrob Agents Chemother
807 49:4754-4756.
808 **58.** Baquero F. 2004. From pieces to patterns: evolutionary engineering in bacterial
809 pathogens. Nat Rev Microbiol 2:510-518
810 **59.** Andersson DI, Balaban NQ, Baquero F, Courvalin P, Glaser P, Gophna U,
811 Kishony R, Molin S, Tønjum T. 2020. Antibiotic resistance: turning evolutionary
812 principles into clinical reality. FEMS Microbiol Rev: fuaa001

60. Jernberg **C**, Löfmark S, Edlund C, Jansson JK. 2010. Long-term impacts of antibiotic exposure on the human intestinal microbiota. Microbiology, 156: 3216-3223

61. Sommer F, Anderson JM, Bharti R, Raes J, Rosenstiel P. 2017. The resilience of the intestinal microbiota influences health and disease. Nat Rev Microbiol 15: 630

62. Novais C, Tedim AP, Lanza VF, Freitas AR, Silveira E, Escada R, Roberts AP, Al-Haroni M, Baquero F, Peixe L, Coque TM. 2016. Co-diversification of *Enterococcus faecium* core genomes and PBP5: evidences of pbp5 horizontal transfer. Front Microbiol 7:1581.

Supplemental Material

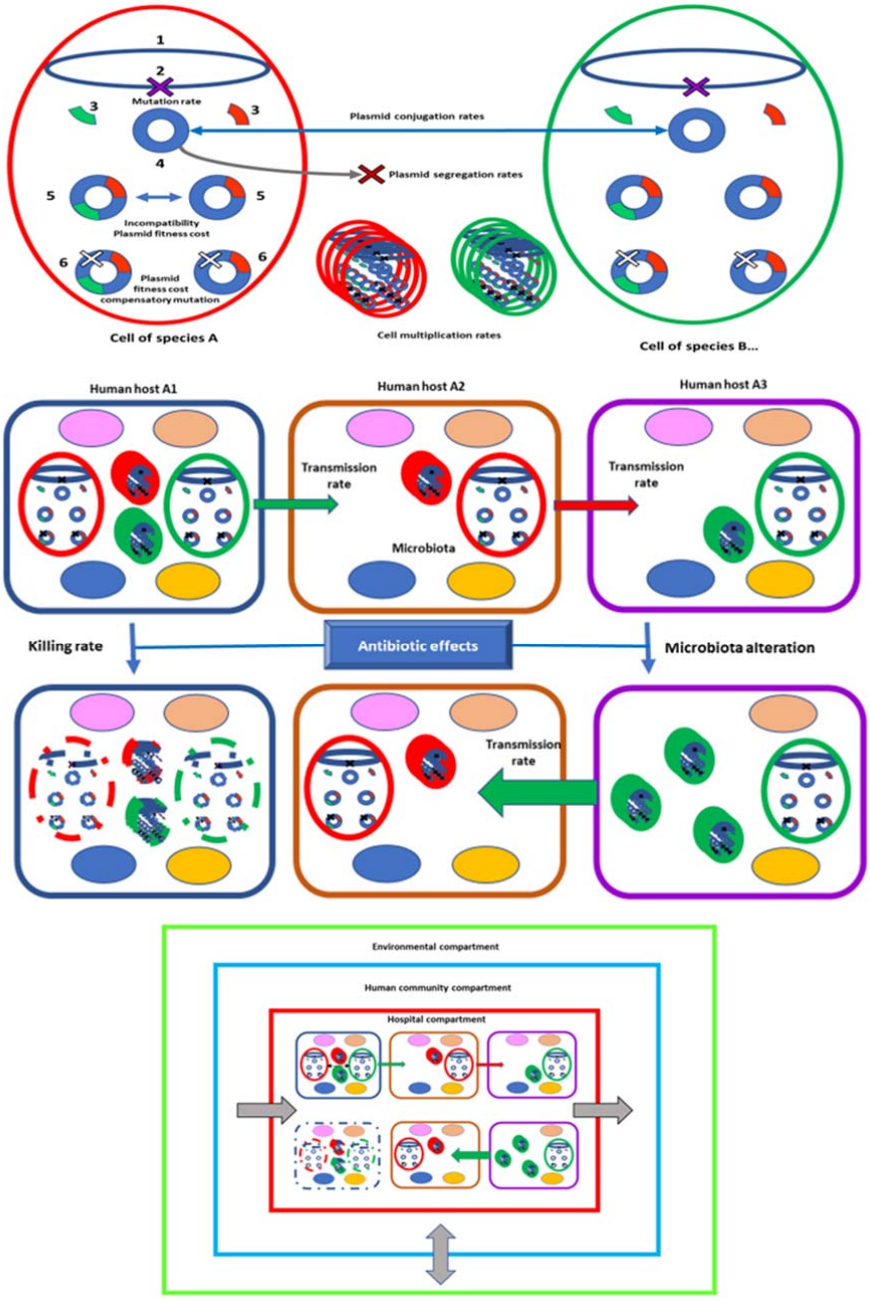

Figure S1. Simplified graphic schema of the membrane computation model. On the top panel, two bacterial cells of the same or different species (red and green circles) containing a

chromosome (black oval, 1), where mutations might occur at variable rates (black X, 2); the absolute number of these cells might be modified. Inside each cell, different antibiotic resistance genes (red, green, 3), that might be harbored in plasmids of the same Inc groups (blue circle crown, 4). Plasmids might compete (incompatibility) inside the cell, eventually leading to the segregation of one of the replicons; also replicons might be submitted to random loss (X, 4), or impose a fitness cost to the host cell (5); however, cost-compensatory mutations can reduce this cost, restoring in part or totally the host-cell replication rate (6). Cells can replicate at different rates (cylinders of red or green ovals). Plasmids can be transferred between cells at different conjugation rates (horizontal black line). On the middle panel, each one of the squares with curved angles correspond to a different human hosts (different colors) where these bacterial cells are established; the colored ovals inside each host correspond (in a simplified way) to the different species in the microbiota. Bacteria harboring plasmids with resistance genes can be transferred from human to human hosts at variable rates (for instance, influenced by hospital hygiene or cross infection). Submitted to antibiotic exposure, different antibiotics can kill (eliminate) bacterial cells at certain rates, but bacteria might survive is they have resistance genes; note that other bacteria of the microbiota can also be eliminated by antibiotics, eventually increasing the population size of the surviving resistant bacteria (as the green cylinders down right), which can be transferred to new hosts. In the lower panel it is depicted that all these processes can occur inside a hospital (red square), or in the human community where the hospital is located (blue square); these compartments are linked by variable admission and discharge rates (horizontal grey arrows) that can also be introduced in the model; finally, the bacterial composition inside the human community is influenced by the interaction with the environment (green square). This figure reveals the multi-nested structure of units involved in antibiotic resistance.